Sustainable Energy & Fuels

Tungsten Oxide-Coated Copper Gallium Selenide Sustains Long-Term Solar Hydrogen Evolution

Journal:	*Sustainable Energy & Fuels*
Manuscript ID	SE-COM-03-2020-000487.R2
Article Type:	Communication
Date Submitted by the Author:	02-Oct-2020
Complete List of Authors:	Palm, David; Stanford University, Chemical Engineering Muzzillo, Christopher; National Renewable Energy Laboratory Ben-Naim, Micha; Stanford University, Chemical Engineering Khan, Imran; National Renewable Energy Laboratory, Materials Science Center Gaillard, Nicolas; University of Hawaii, Jaramillo, Thomas; Stanford University, Assistant Professor of Chemical Engineering

Tungsten Oxide-Coated Copper Gallium Selenide Sustains Long-Term Solar Hydrogen Evolution

David W. Palm,[†] Christopher P. Muzzillo,[‡] Micha Ben-Naim,[†] Imran Khan,[‡] Nicolas Gaillard,[§] Thomas F. Jaramillo[†∥]

[†]Department of Chemical Engineering, Stanford University, 443 Via Ortega, Stanford, California 94305, United States

[‡]National Renewable Energy Laboratory, 15013 Denver W Pkwy, Golden, Colorado 80401, United States

[§]Hawaii Natural Energy Institute (HNEI), University of Hawaii, 1680 East−West Rd POST 109, Honolulu, Hawaii 96822, United States

[∥]SUNCAT Center for Interface Science and Catalysis, SLAC National Accelerator Laboratory, 2575 Sand Hill Road, Menlo Park, California 94025, United States

Abstract

This work demonstrates that ultrathin (4 nm) tungsten oxide (WO_3) coatings on copper gallium selenide ($CuGa_3Se_5$) photocathodes have the potential for long-term solar hydrogen evolution. With a combination of a robust 1.84-eV $CuGa_3Se_5$ absorber layer, a WO_3 protective coating, and a Pt catalyst, we obtain a new durability milestone for any non-silicon photoelectrochemical hydrogen-producing device by passing 21,490 C cm^{-2} of charge across six weeks of continuously-illuminated chronoamperometric testing under applied bias.

Text

One approach to storing the vast but variable solar resource is to use integrated solar-driven, hydrogen fuel-producing devices in a process called solar water splitting.[1] A key challenge for these systems has been demonstrating technologically-relevant durability in the corrosive aqueous environments required for their operation.[2] Few semiconductors with high solar energy conversion efficiency have demonstrated intrinsic chemical stability while exposed to water under illumination. As a result, a common approach for solar water splitting devices involves physically isolating the light absorbing material from the electrolyte using a coating, while maintaining good optical transmittance and electrical conductivity through this layer.[3–5] For the hydrogen-evolving half-cell, studies have shown continuous operation for longer than ten days either by employing titanium dioxide (TiO_2) or molybdenum disulfide (MoS_2) coatings on silicon absorbers[6–8] or by constructing their photoactive junction using a semiconducting material that achieves long-term operability in contact with the electrolyte.[9–13]

In seeking to fabricate a photoelectrochemical (PEC) device with high theoretical efficiency for water splitting and long-term operational durability, we identified the p-type chalcopyrite-like, ordered vacancy compound material copper gallium selenide ($CuGa_3Se_5$) as a candidate absorber for several reasons: 1) given that its 1.84 eV band gap is wider than that of many state-of-the-art chalcopyrite PEC absorbers,[9,11,22–26,14–21] it has the potential to produce the >1 V photovoltage required to enable efficient tandem unassisted water splitting devices when paired with a narrow bandgap absorber; 2) it has achieved greater than 10 mA cm^{-2} in PEC hydrogen evolution under 1 sun illumination,[12] another requirement for high-efficiency devices; and 3) it has shown impressive durability under operation in aqueous electrolyte.[12,27]

While capping layers such as CdS,[9–11,15–17] TiO_2,[20,21] AZO/TiO_2,[18] Al_2O_3/TiO_2,[19] In_2S_3,[22] ZnS,[27,28] ZnO,[24] TiO_2/MoS_2,[26] and Ti/Mo[29,30] have been applied in chalcopyrite-based photocathode devices, only CdS, ZnS, and Ti/Mo coatings have enabled greater than 24 h of illuminated hydrogen-evolving operation,[9–11,17,27] and only in near-neutral electrolyte conditions that may prove unsuitable from a device engineering perspective. Alternatively, we hypothesized that pairing a $CuGa_3Se_5$ absorber with a coating of tungsten oxide (WO_3) would yield a device that is highly durable and high-performing. WO_3 is predicted to have good chemical stability in acidic environments[31] and limited absorption of visible light (due to its indirect E_g = 2.7 eV band gap),[32] motivating the study herein.

Drawing inspiration from the development of ultrathin TiO_2 protective coatings,[33] this work demonstrates the use of ultrathin WO_3 coatings as a new strategy for enabling long-term durability in solar hydrogen production, with the potential for utility in other acidic-media electrocatalytic reactions. While previous workers have utilized bulk n-type WO_3 as a heterojunction partner with p-type semiconductor photocathodes without addressing the long-term operation of these devices,[32,34,35] this work explores the durability advantages of WO_3 coatings.

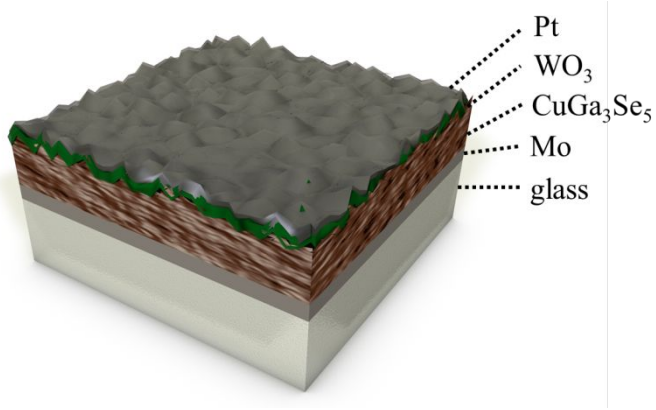

Scheme 1: $CuGa_3Se_5$|WO_3|Pt photocathode device

Ultrathin WO_3 coatings were synthesized via pulsed chemical vapor deposition[36] onto $CuGa_3Se_5$ absorbers that had been co-evaporated on molybdenum-coated soda-lime glass substrates,[12] as shown in Scheme 1. The thickness of the WO_3 coatings was 3.8 nm, as determined by spectroscopic ellipsometry of the film synthesized on a silicon wafer substrate during the same deposition. Grazing incidence x-ray diffraction (GI-XRD) measurements were unable to detect signal from the ultrathin WO_3 coatings (Figure S1), indicating that the as-prepared films are either not sufficiently crystalline or too thin to yield detectable diffraction patterns in this instrument. The WO_3-coated samples were then loaded with a nanoparticulate platinum layer by electron beam evaporation, as the hydrogen-evolving catalyst. Both the WO_3 and Pt coatings were shown to be uniformly distributed over the entire $CuGa_3Se_5$ substrate as measured by scanning electron microscopy and energy-dispersive x-ray (SEM-EDX) elemental mapping (Figure 1). Cross-sectional SEM measurements were not sensitive enough to differentiate the ultrathin WO_3/Pt layers from the underlying absorber (Figure S2) but appear to show conformal surface coverage of the $CuGa_3Se_5$ crystallites with these coatings (Figure S2c). These coatings were also shown to transmit a majority of the simulated solar flux, as demonstrated by UV/Vis transmittance measurements (Figure S3).

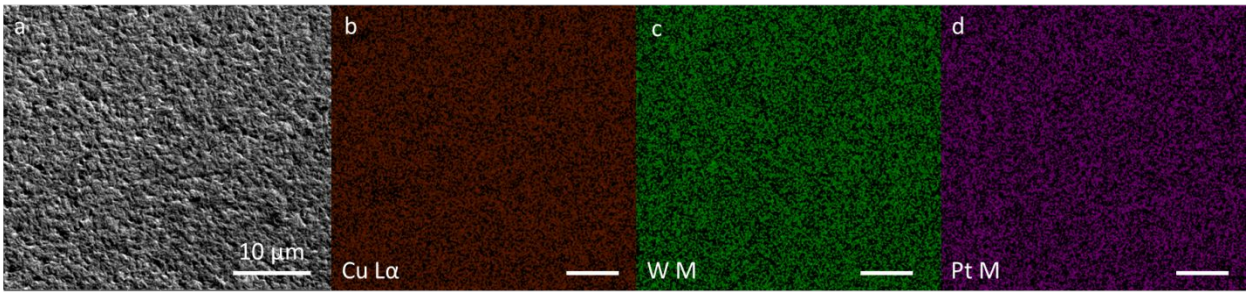

Figure 1: (a) SEM image of an as-prepared $CuGa_3Se_5|WO_3|Pt$ device and associated EDX elemental maps of the Cu Lα (b), W M (c), and Pt M (d) signals; all of the scale bars are 10 μm in length.

The activity and durability of these photocathodes for the hydrogen evolution reaction (HER) under continuous simulated 1 Sun AM1.5G illumination were investigated via linear sweep voltammetry (LSV) and chronoamperometry (CA), respectively (Figure 2). As determined from the LSV data displayed in Figure 2a, the $CuGa_3Se_5|WO_3|Pt$ photocathode generated a saturation photocurrent density of -8.5 mA cm^{-2} and a photocurrent onset potential (as defined previously[26] and determined in Figure S4) of E = +0.32 V *vs*. RHE compared to -8.1 mA cm^{-2} and +0.30 V *vs*. RHE for the bare $CuGa_3Se_5$ photocathode. A separate $CuGa_3Se_5|Pt$ photocathode shows an improved onset potential (+0.39 V *vs*. RHE) compared to the bare $CuGa_3Se_5$ photocathode (Figure S5) due to the improved catalysis of the Pt catalyst compared to the bare $CuGa_3Se_5$ surface. However, the $CuGa_3Se_5|WO_3|Pt$ photocathode has an onset potential 0.07 V lower than that of the $CuGa_3Se_5|Pt$ photocathode, apparently due to a suboptimal $CuGa_3Se_5|WO_3$ interface. Indeed, we predict there is room for improvement at this interface, since the idealized band energy diagrams for the $CuGa_3Se_5|WO_3|Pt$ device (Figure S6) indicate the possibility of achieving photovoltage exceeding 0.5 V from an ideal $CuGa_3Se_5/WO_3$ heterojunction device.[12,37,38] The complicated effects of the Pt catalyst and WO_3 coating on the onset potential provide motivation for a quantitative investigation of the system's interfacial energetics involving multi-modal spectroscopies[39,40] that are, however, outside of the scope of the current work.

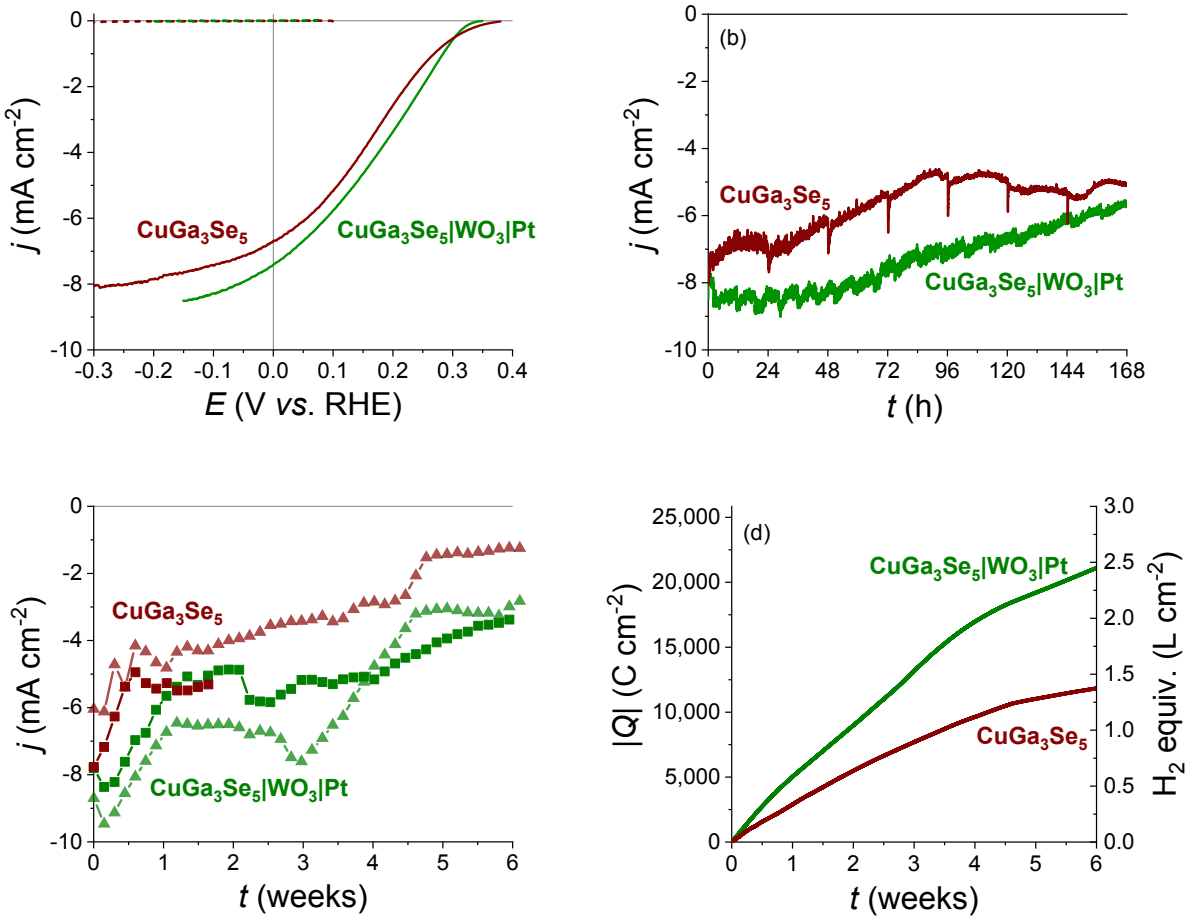

Figure 2: (a) PEC LSV of a bare $CuGa_3Se_5$ photocathode (maroon) and a $CuGa_3Se_5|WO_3|Pt$ photocathode (green); LSV with the light blanked ('dark LSV') shown in dashed lines, which track the $j = 0$ axis; (b) PEC CA of the same photocathodes over the first week of operation at potentials of -0.3 V *vs*. RHE (bare $CuGa_3Se_5$) and -0.15 V *vs*. RHE ($CuGa_3Se_5|WO_3|Pt$); (c) long-term CA of the same photocathodes (maroon squares and green squares) along with duplicates of each electrode type (pale maroon triangles and pale green triangles, E_{CA}=-0.2 V and -0.25 V *vs*. RHE, respectively)—here the lines are solely guides for the eye to connect the one daily data point shown; (d) integrated charge passed by a $CuGa_3Se_5|WO_3|Pt$ photocathode (green) and a bare $CuGa_3Se_5$ photocathode (maroon) over six weeks of CA testing, with the secondary vertical axis representing the equivalent volume of H_2 (at P =1 atm) that would be produced by this amount of charge; all experiments were performed in 0.5 M H_2SO_4 electrolyte purged with H_2 gas, utilizing a $Hg/HgSO_4$ reference electrode and an Ir/IrO_x counter electrode, with light experiments performed under continuous simulated 1 Sun AM1.5G illumination.

The photocurrent densities and onset potentials measured here are commensurate with those reported for other photocathodes employing $CuGa_3Se_5$ as absorber. In previous studies, the maximum photocurrent densities under simulated 1 Sun AM 1.5G illumination range from -5 mA cm^{-2} to -10.4 mA cm^{-2}, and the onset potentials range from +0.1 V *vs*. RHE with a bare $CuGa_3Se_5$ photocathode to +0.35 V *vs*. RHE with a Pt-catalyzed $CuGa_3Se_5$ photocathode.[12,41] With these studies for context, we will demonstrate further below that we were able to achieve milestone durability targets utilizing $CuGa_3Se_5$ photocathodes that approach state-of-the-art performance. We aim to develop strategies for stability that can continue to be

leveraged as $CuGa_3Se_5$ photocathodes approach ideality. As a single-junction device employing a 1.84 eV band gap absorber, a $CuGa_3Se_5$ photocathode can generate a theoretical maximum photocurrent density of -18.5 mA cm^{-2} under 1 Sun AM 1.5G illumination[42–44] and a theoretical photovoltage exceeding 1 V. The disparity between our photocathode activity and that of an ideal $CuGa_3Se_5$ photocathode could result from several factors, including: 1) the possibility of phase impurities in the absorber layer that could lead to recombination in the film that may limit the saturation photocurrent density, as discussed in previous work,[12] and 2) the absence of an interfacial buffer layer, *i.e.* a non-ideal junction between the $CuGa_3Se_5$ absorber and the applied overlayers that may suppress the demonstrated onset potential.

For chronoamperometric durability testing, each photocathode device was operated under continuous simulated 1 Sun illumination at a potential where its photocurrent density approaches its saturation value. Since this bias condition induces the maximum amount of charge to be passed through the PEC device, we note that this is a strenuous durability testing protocol, while recognizing the importance of standardizing durability testing within the solar hydrogen production community. Whereas the photocurrent density of the bare $CuGa_3Se_5$ photocathode immediately began to decrease from its initial value (-8.0 mA cm^{-2}), the $CuGa_3Se_5|WO_3|Pt$ photocathode was able to maintain its initial photocurrent density (-8.1 mA cm^{-2}) for 67 h of operation during the CA durability experiment (Figure 2b). This improved stability indicates that the $WO_3|Pt$ coating plays a substantial role in sustaining effective solar-driven hydrogen production over these initial stages of the experiment. This notion is supported by the fact that the durability of a Pt-coated $CuGa_3Se_5$ photocathode without any WO_3 coating is significantly worse than either the $CuGa_3Se_5|WO_3|Pt$ or bare $CuGa_3Se_5$ photocathode over a week of testing (Figure S7). Furthermore, a degenerately doped n-type Si conductive substrate coated with WO_3 and Pt ($n^+Si|WO_3|Pt$, an HER electrocatalytic analogue electrode) maintained reasonable activity over 40 h of continuous operation at -10 mA cm^{-2}, whereas a $n^+Si|Pt$ device without WO_3 coating degraded rapidly within 3 h of testing (Figure S8), demonstrating that the WO_3 coating also plays a role in extending durability in this case.

Ultimately, the aforementioned $CuGa_3Se_5|WO_3|Pt$ photocathode, another identically processed $CuGa_3Se_5|WO_3|Pt$ photocathode, and a bare $CuGa_3Se_5$ photocathode all sustained light-driven hydrogen evolution for over 6 weeks of continuous operation under applied bias (Figure 2c and Figure S9). Figure 2d compares the cumulative charge passed as a function of time for the most-durable $CuGa_3Se_5|WO_3|Pt$ device (pale green data in Figure 2c) to that of a bare $CuGa_3Se_5$ device (pale maroon data in Figure 2c); the experiments resulted in passing 21,490 C cm^{-2} and 12,590 C cm^{-2} of charge, respectively. In fact, both of the $CuGa_3Se_5|WO_3|Pt$ photocathodes surpassed the previous durability milestone (in C cm^{-2}) for any non-silicon solar hydrogen-producing device (Figure S9c) by generating 21,490 C cm^{-2} and 19,510 C cm^{-2}, respectively.[5,12] Table 1 contains a comparison of durability results calculated from literature reports of Cu chalcopyrite photocathodes, which have demonstrated the best durability of any non-silicon devices.

Table 1: Comparison of most-durable Cu chalcopyrite photocathodes

Absorber	Coating	pH	*t* (days)	*Q* (C cm^{-2})	ref.
$CuGaSe_2$	CdS	7	12	3400	Moriya, 2013
$(Ag,Cu)GaSe_2|CuGa_3Se_5$	CdS|Pt	7	20	12900	Zhang, 2015
$Cu(In,Ga)Se_2$	CdS|Ti|Mo|Pt	6.8	10	16300	Kumagai, 2015
$CuGa_3Se_5$	none	0.3	17	11750	Muzzillo, 2018
$CuGa_3Se_5$	none	0.3	48	12590	*this work*
$CuGa_3Se_5$	$WO_3|Pt$	0.3	44	21490, 19510	*this work*

For insight into morphological, chemical, and structural changes undergone by the device during PEC durability testing, SEM-EDX (Figures 3, 4, and S10) and GI-XRD (Figure S11) analyses were conducted on the $CuGa_3Se_5|WO_3|Pt$ photocathode after six weeks of testing. Table 2 presents the atomic concentration of the $CuGa_3Se_5|WO_3|Pt$ photocathodes as-prepared and after six weeks of durability testing, quantified from the EDX spectra in Figure 4. The most notable changes in composition over the course of testing are the dramatic increase in the Cu signal relative to the Ga and Se signals, the significant decrease in signal from Pt, and the absence of W signal after testing. The SEM image in Figure 3a reveals dramatic changes to the sample surface over the course of extended PEC testing, and the EDX mapping shows that in contrast to previously uniform distribution, Cu-rich regions appear in a striated pattern after testing (Figure 3b). EDX mapping of the Ga and Se signals from this same sample reveals that the Cu-poor regions are enriched in Ga and Se, and vice versa (Figure S10). The GI-XRD analysis indicate that the crystalline component of the $CuGa_3Se_5$ absorber layer remains largely unchanged before and after long-term operation of the $CuGa_3Se_5$ and the $CuGa_3Se_5|WO_3|Pt$ devices, and no signal was detected from the WO_3 or Pt overlayers either before or after testing (Figure S11a). The appearance of a new peak near $2\theta = 25°$ after testing in the $CuGa_3Se_5|WO_3|Pt$ device is best attributed to the formation of a crystalline phase resembling Cu_3Se_2. As reported previously,[12] this feature is not present in the tested bare $CuGa_3Se_5$ device (Figure S11b), indicating that the $WO_3|Pt$ coating may play a role in the stabilization or formation of this phase.

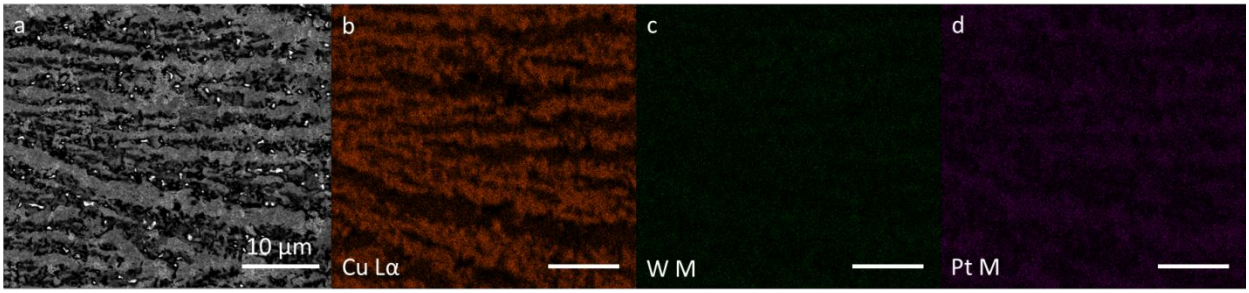

Figure 3: (a) SEM image of a $CuGa_3Se_5|WO_3|Pt$ photocathode after six weeks of PEC durability testing, and associated EDX elemental maps of the Cu Lα (b), W M (c), and Pt M (d) signals; all of the scale bars are 10 µm in length.

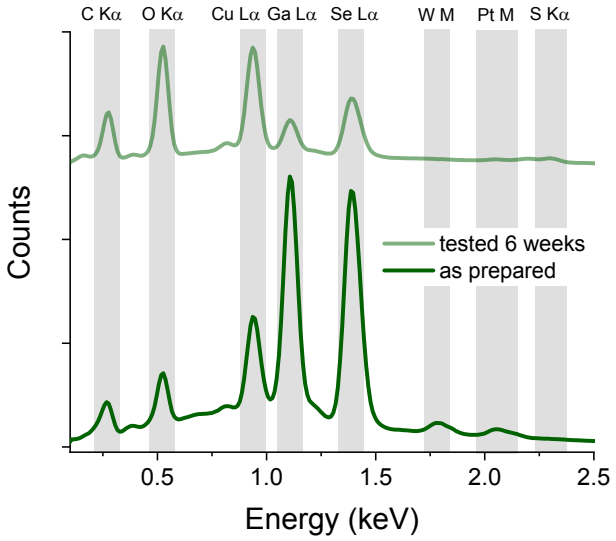

Figure 4: EDX spectra of an as-prepared $CuGa_3Se_5|WO_3|Pt$ photocathode (green) and a $CuGa_3Se_5|WO_3|Pt$ photocathode that had undergone six weeks of PEC durability testing (pale green)

Table 2: Atomic concentration quantified from EDX analysis; with an accelerating voltage of 3 keV, the interaction volume for the technique does not include the entire thickness of the $CuGa_3Se_5$ layer

Device	Sample	Cu %	Ga %	Se %	W %	Pt %
$CuGa_3Se_5\|WO_3\|Pt$	as prepared	12.2	36.7	48.5	0.9	1.7
$CuGa_3Se_5\|WO_3\|Pt$	tested 6 weeks	52.4	16.0	31.1	0	0.5

Given the evolution of the Cu:Ga:Se ratio in the absorber film and drawing on previous work demonstrating the dissolution of Cu from copper gallium selenide photocathodes in acidic media,[45] it is evident that the key contributor to diminishing photoactivity in these devices is dissolution of the constituent elements from the absorber film. The presented data lead to at least two general pathways for the degradation by dissolution: 1) the WO_3 and Pt coatings themselves dissolve over the course of extended durability testing, followed by dissolution of the exposed $CuGa_3Se_5$, and 2) the $CuGa_3Se_5$ absorber dissolves through pin holes in the WO_3 and Pt coatings, ultimately compromising the mechanical integrity of the WO_3 and Pt overlayers. We propose that the ultrathin WO_3 coating employed in this study is extending the durability of these photocathodes by decreasing the rate of dissolution of the $CuGa_3Se_5$ absorber by mitigating its exposure to the corrosive electrolyte. Future work on WO_3 coating of $CuGa_3Se_5$ absorbers will involve both optimizing the deposition and investigating the mechanical and (electro)chemical stability of the WO_3 coatings, especially given the possibility of phase change occurring in the material under the present operating conditions.[31] Given the relative increase in Cu content within the information depth probed by this EDX measurement, it is evident that the net rate of Ga and Se dissolution is greater than the net rate of Cu dissolution under the photoreductive operating conditions of the durability test. Investigating these kinetics of dissolution from photoelectrode absorbers and coatings through methods such as inductively-couple mass spectrometry is an important area of method development.[46]

Importantly, we note that the vast majority of the observed charge passed over this extended time scale is due to solar hydrogen evolution rather than parasitic processes that occur without light impetus (supporting calculations are presented in the Electronic Supporting Information). This point is evidenced in several ways: (i) the initial 'dark LSV' for all photocathodes shows a current response that nearly overlaps the $j = 0$ axis (Figure 2a), (ii) the current densities of the $CuGa_3Se_5|WO_3|Pt$ devices decrease by an order of magnitude (to -0.11 and -0.26 mA cm^{-2}, respectively) when the lamp is blanked at the end of the durability tests (Figure S9a), and (iii) hydrogen bubbles were seen forming and detaching from the electrode surface for the duration of the experiment. Developing methods for collecting and quantifying hydrogen over the course of long-term durability testing is a recognized need for the solar hydrogen community.[6,7,50,8–12,47–49]

In this communication, we demonstrate the utility of $CuGa_3Se_5$ absorbers coated with ultrathin WO_3 coatings for long-term operation of solar-driven hydrogen production and achieve a new durability milestone for any non-silicon photocathode device, passing 21,490 C cm^{-2} of charge over six weeks of continuously illuminated testing under applied bias. Since solar cell devices based upon $CuGa_3Se_5$ absorbers have generated open-circuit voltages exceeding 0.75 V by employing interfacial buffer layers such as CdS,[12] there is great opportunity to adapt the durability strategies developed herein to $CuGa_3Se_5$ photocathode devices that exceed the maximum +0.39 V *vs*. RHE onset potential demonstrated in this work. With the incorporation of such a buffer layer and further optimization of the WO_3 deposition process, this system has the potential to reach technologically relevant activity and durability for a wide band gap photocathode. These WO_3 coatings, in turn, have the potential to be widely applicable in extending the durability of solar-driven hydrogen-evolving systems toward meaningful technological timeframes.

Electronic Supporting Information. Experimental details, materials synthesis and characterization, as well as calibration and data analysis methodologies, are included in the Electronic Supporting Information. Normalized data for the electrochemical experiments are included in an .xls file included as Electronic Supporting Information.

Acknowledgements

The authors gratefully acknowledge research support from the HydroGEN Advanced Water Splitting Materials Consortium, established as part of the Energy Materials Network under the U.S. Department of Energy, Office of Energy Efficiency and Renewable Energy, Hydrogen and Fuel Cell Technologies Office, under Contract DE-EE0006670 administrated by the University of Hawaii. This work was authored in part by the National Renewable Energy Laboratory, operated by Alliance for Sustainable Energy, LLC, for the U.S. DOE under Contract No. DE-AC36-08GO28308. Funding provided by the U.S. Department of Energy Office of Energy Efficiency and Renewable Energy. The views expressed in the article do not necessarily represent the views of the DOE or the U.S. Government. The U.S. Government retains and the publisher, by accepting the article for publication, acknowledges that the U.S. Government retains a nonexclusive, paid-up, irrevocable, worldwide license to publish or reproduce the published form of this work, or allow others to do so, for U.S. Government purposes. Materials characterization contained in this work was performed at the Stanford Nano Shared Facilities (SNSF), supported by the National Science Foundation under Award ECCS-1542152. Coating depositions were

conducted at the Stanford Nanofabrication Facility (SNF) with guidance from the team there, especially staff scientist Dr. Michelle Rincon and lab member Dr. J. Provine. Thanks to Alex DeAngelis and Dr. Ivan Moreno-Hernandez for discussions leading to the development of the coating strategy presented here, and to Dr. James Young for a discussion of best practices in PEC durability testing. Thanks to Dr. Pongkarn Chakthranont for contributing the three-dimensional device schematic and Joel Sanchez for help in adapting it. Finally, D.W.P. would like to thank the National Science Foundation for its support through the Graduate Research Fellowship Program.

References

(1) Fujishima, A.; Honda, K. Electrochemical Photolysis of Water at a Semiconductor Electrode. *Nature* **1972**, *238* (5358), 37–38. https://doi.org/10.1038/238037a0.

(2) Walter, M. G.; Warren, E. L.; McKone, J. R.; Boettcher, S. W.; Mi, Q.; Santori, E. a; Lewis, N. S. Solar Water Splitting Cells. *Chem. Rev.* **2010**, *110* (11), 6446–6473. https://doi.org/10.1021/cr1002326.

(3) Hu, S.; Lewis, N. S.; Ager, J. W.; Yang, J.; McKone, J. R.; Strandwitz, N. C. Thin-Film Materials for the Protection of Semiconducting Photoelectrodes in Solar-Fuel Generators. *J. Phys. Chem. C* **2015**, *119* (43), 24201–24228. https://doi.org/10.1021/acs.jpcc.5b05976.

(4) Guijarro, N.; Prévot, M. S.; Sivula, K. Surface Modification of Semiconductor Photoelectrodes. *Phys. Chem. Chem. Phys.* **2015**, *17* (24), 15655–15674. https://doi.org/10.1039/C5CP01992C.

(5) Bae, D.; Seger, B.; Vesborg, P. C. K.; Hansen, O.; Chorkendorff, I. Strategies for Stable Water Splitting via Protected Photoelectrodes. *Chem. Soc. Rev.* **2017**, *46* (7), 1933–1954. https://doi.org/10.1039/C6CS00918B.

(6) Seger, B.; Tilley, D. S.; Pedersen, T.; Vesborg, P. C. K.; Hansen, O.; Grätzel, M.; Chorkendorff, I. Silicon Protected with Atomic Layer Deposited TiO2: Durability Studies of Photocathodic H2 Evolution. *RSC Adv.* **2013**, *3* (48), 25902. https://doi.org/10.1039/c3ra45966g.

(7) King, L. A.; Hellstern, T. R.; Park, J.; Sinclair, R.; Jaramillo, T. F. Highly Stable Molybdenum Disulfide Protected Silicon Photocathodes for Photoelectrochemical Water Splitting. *ACS Appl. Mater. Interfaces* **2017**, *9* (42), 36792–36798. https://doi.org/10.1021/acsami.7b10749.

(8) Bae, D.; Seger, B.; Hansen, O.; Vesborg, P. C. K.; Chorkendorff, I. Durability Testing of Photoelectrochemical Hydrogen Production under Day/Night Light Cycled Conditions. *ChemElectroChem* **2019**, *6* (1), 106–109. https://doi.org/10.1002/celc.201800918.

(9) Moriya, M.; Minegishi, T.; Kumagai, H.; Katayama, M.; Kubota, J.; Domen, K. Stable Hydrogen Evolution from CdS-Modified CuGaSe 2 Photoelectrode under Visible-Light Irradiation. *J. Am. Chem. Soc.* **2013**, *135* (10), 3733–3735. https://doi.org/10.1021/ja312653y.

(10) Zhang, L.; Minegishi, T.; Nakabayashi, M.; Suzuki, Y.; Seki, K.; Shibata, N.; Kubota, J.; Domen, K. Durable Hydrogen Evolution from Water Driven by Sunlight Using (Ag,Cu)GaSe 2 Photocathodes Modified with CdS and CuGa 3 Se 5. *Chem. Sci.* **2015**, *6* (2), 894–901. https://doi.org/10.1039/C4SC02346C.

(11) Kumagai, H.; Minegishi, T.; Sato, N.; Yamada, T.; Kubota, J.; Domen, K. Efficient Solar Hydrogen Production from Neutral Electrolytes Using Surface-Modified Cu(In,Ga)Se 2 Photocathodes. *J. Mater. Chem. A* **2015**, *3* (16), 8300–8307. https://doi.org/10.1039/C5TA01058F.

(12) Muzzillo, C. P.; Klein, W. E.; Li, Z.; DeAngelis, A. D.; Horsley, K.; Zhu, K.; Gaillard, N. Low-Cost, Efficient, and Durable H 2 Production by Photoelectrochemical Water Splitting with CuGa 3 Se 5 Photocathodes. *ACS Appl. Mater. Interfaces* **2018**, *10* (23), 19573–19579. https://doi.org/10.1021/acsami.8b01447.

(13) Wang, Y.; Wu, Y.; Schwartz, J.; Sung, S. H.; Hovden, R.; Mi, Z. A Single-Junction Cathodic Approach for Stable Unassisted Solar Water Splitting. *Joule* **2019**, *3* (10), 2444–2456. https://doi.org/10.1016/j.joule.2019.07.022.

(14) Marsen, B.; Cole, B.; Miller, E. L. Photoelectrolysis of Water Using Thin Copper Gallium Diselenide Electrodes. *Sol. Energy Mater. Sol. Cells* **2008**, *92* (9), 1054–1058. https://doi.org/10.1016/j.solmat.2008.03.009.

(15) Kumagai, H.; Minegishi, T.; Moriya, Y.; Kubota, J.; Domen, K. Photoelectrochemical Hydrogen Evolution from Water Using Copper Gallium Selenide Electrodes Prepared by a Particle Transfer Method. *J. Phys. Chem. C* **2014**, *118* (30), 16386–16392. https://doi.org/10.1021/jp409921f.

(16) Septina, W.; Gunawan; Ikeda, S.; Harada, T.; Higashi, M.; Abe, R.; Matsumura, M. Photosplitting of Water from Wide-Gap Cu(In,Ga)S 2 Thin Films Modified with a CdS Layer and Pt Nanoparticles for a High-Onset-Potential Photocathode. *J. Phys. Chem. C* **2015**, *119* (16), 8576–8583. https://doi.org/10.1021/acs.jpcc.5b02068.

(17) Zhang, L.; Minegishi, T.; Kubota, J.; Domen, K. Hydrogen Evolution from Water Using AgxCu1−xGaSe2 Photocathodes under Visible Light. *Phys. Chem. Chem. Phys.* **2014**, *16* (13), 6167. https://doi.org/10.1039/c3cp54590c.

(18) Luo, J.; Tilley, S. D.; Steier, L.; Schreier, M.; Mayer, M. T.; Fan, H. J.; Grätzel, M. Solution Transformation of Cu 2 O into CuInS 2 for Solar Water Splitting. *Nano Lett.* **2015**, *15* (2), 1395–1402. https://doi.org/10.1021/nl504746b.

(19) Chen, M.; Liu, Y.; Li, C.; Li, A.; Chang, X.; Liu, W.; Sun, Y.; Wang, T.; Gong, J. Spatial Control of Cocatalysts and Elimination of Interfacial Defects towards Efficient and Robust CIGS Photocathodes for Solar Water Splitting. *Energy Environ. Sci.* **2018**, *11* (8), 2025–2034. https://doi.org/10.1039/C7EE03650G.

(20) Zhao, J.; Minegishi, T.; Zhang, L.; Zhong, M.; Gunawan; Nakabayashi, M.; Ma, G.; Hisatomi, T.; Katayama, M.; Ikeda, S.; et al. Enhancement of Solar Hydrogen Evolution from Water by Surface Modification with CdS and TiO 2 on Porous CuInS 2 Photocathodes Prepared by an Electrodeposition-Sulfurization Method. *Angew. Chemie Int. Ed.* **2014**, *53* (44), 11808–11812. https://doi.org/10.1002/anie.201406483.

(21) Guijarro, N.; Prévot, M. S.; Yu, X.; Jeanbourquin, X. A.; Bornoz, P.; Bourée, W.; Johnson, M.; Le Formal, F.; Sivula, K. A Bottom-Up Approach toward All-Solution-Processed High-Efficiency Cu(In,Ga)S 2 Photocathodes for Solar Water Splitting. *Adv. Energy Mater.* **2016**, *6* (7), 1501949. https://doi.org/10.1002/aenm.201501949.

(22) Gunawan; Septina, W.; Ikeda, S.; Harada, T.; Minegishi, T.; Domen, K.; Matsumura, M. Platinum and Indium Sulfide-Modified CuInS 2 as Efficient Photocathodes for Photoelectrochemical Water Splitting. *Chem. Commun.* **2014**, *50* (64), 8941. https://doi.org/10.1039/C4CC03634D.

(23) Mali, M. G.; Yoon, H.; Joshi, B. N.; Park, H.; Al-Deyab, S. S.; Lim, D. C.; Ahn, S.; Nervi, C.; Yoon, S. S. Enhanced Photoelectrochemical Solar Water Splitting Using a Platinum-Decorated CIGS/CdS/ZnO Photocathode. **2015**.

(24) Jacobsson, T. J.; Platzer-Björkman, C.; Edoff, M.; Edvinsson, T. CuInxGa1−xSe2 as an Efficient

Photocathode for Solar Hydrogen Generation. *Int. J. Hydrogen Energy* **2013**, *38* (35), 15027–15035. https://doi.org/10.1016/j.ijhydene.2013.09.094.

(25) Ikeda, S.; Nakamura, T.; Lee, S. M.; Yagi, T.; Harada, T.; Minegishi, T.; Matsumura, M. Photoreduction of Water by Using Modified CuInS2 Electrodes. *ChemSusChem* **2010**, *4* (2), n/a-n/a. https://doi.org/10.1002/cssc.201000169.

(26) Hellstern, T. R.; Palm, D. W.; Carter, J.; DeAngelis, A. D.; Horsley, K.; Weinhardt, L.; Yang, W.; Blum, M.; Gaillard, N.; Heske, C.; et al. Molybdenum Disulfide Catalytic Coatings via Atomic Layer Deposition for Solar Hydrogen Production from Copper Gallium Diselenide Photocathodes. *ACS Appl. Energy Mater.* **2019**, *2* (2), 1060–1066. https://doi.org/10.1021/acsaem.8b01562.

(27) Kim, J.; Minegishi, T.; Kobota, J.; Domen, K. Enhanced Photoelectrochemical Properties of CuGa 3 Se 5 Thin Films for Water Splitting by the Hydrogen Mediated Co-Evaporation Method. *Energy Environ. Sci.* **2012**, *5* (4), 6368–6374. https://doi.org/10.1039/C1EE02280F.

(28) Kageshima, Y.; Minegishi, T.; Goto, Y.; Kaneko, H.; Domen, K. Particulate Photocathode Composed of (ZnSe) 0.85 (CuIn 0.7 Ga 0.3 Se 2) 0.15 Synthesized with Na 2 S for Enhanced Sunlight-Driven Hydrogen Evolution. *Sustain. Energy Fuels* **2018**, *2* (9), 1957–1965. https://doi.org/10.1039/C8SE00101D.

(29) Higashi, T.; Kaneko, H.; Minegishi, T.; Kobayashi, H.; Zhong, M.; Kuang, Y.; Hisatomi, T.; Katayama, M.; Takata, T.; Nishiyama, H.; et al. Overall Water Splitting by Photoelectrochemical Cells Consisting of (ZnSe) 0.85 (CuIn 0.7 Ga 0.3 Se 2) 0.15 Photocathodes and BiVO 4 Photoanodes. *Chem. Commun.* **2017**. https://doi.org/10.1039/C7CC06637F.

(30) Kaneko, H.; Minegishi, T.; Nakabayashi, M.; Shibata, N.; Kuang, Y.; Yamada, T.; Domen, K. A Novel Photocathode Material for Sunlight-Driven Overall Water Splitting: Solid Solution of ZnSe and Cu(In,Ga)Se 2. *Adv. Funct. Mater.* **2016**, *26* (25), 4570–4577. https://doi.org/10.1002/adfm.201600615.

(31) Pourbaix, M. *Atlas of Electrochemical Equilibria in Aqueous Solutions*, 1st Englis.; New York, 1966.

(32) Yoon, K. H.; Shin, C. W.; Kang, D. H. Photoelectrochemical Conversion in a WO3 Coated P-Si Photoelectrode: Effect of Annealing Temperature. *J. Appl. Phys.* **1997**, *81* (10), 7024–7029. https://doi.org/10.1063/1.365268.

(33) Chen, Y. W.; Prange, J. D.; Dühnen, S.; Park, Y.; Gunji, M.; Chidsey, C. E. D.; McIntyre, P. C. Atomic Layer-Deposited Tunnel Oxide Stabilizes Silicon Photoanodes for Water Oxidation. *Nat. Mater.* **2011**, *10* (7), 539–544. https://doi.org/10.1038/nmat3047.

(34) Yoon, K. H.; Lee, J. W.; Cho, Y. S.; Kang, D. H. Photoeffects in WO 3 /GaAs Electrode. *J. Appl. Phys.* **1996**, *80* (12), 6813–6818. https://doi.org/10.1063/1.363810.

(35) Yoon, K. H.; Seo, D. K.; Cho, Y. S.; Kang, D. H. Effect of Pt Layers on the Photoelectrochemical Properties of a WO3/p-Si Electrode. *J. Appl. Phys.* **1998**, *84* (7), 3954–3959. https://doi.org/10.1063/1.368573.

(36) Liu, R.; Lin, Y.; Chou, L.-Y.; Sheehan, S. W.; He, W.; Zhang, F.; Hou, H. J. M.; Wang, D. Water Splitting by Tungsten Oxide Prepared by Atomic Layer Deposition and Decorated with an Oxygen-Evolving Catalyst. *Angew. Chemie* **2011**, *123* (2), 519–522. https://doi.org/10.1002/ange.201004801.

(37) Bär, M.; Weinhardt, L.; Marsen, B.; Cole, B.; Gaillard, N.; Miller, E.; Heske, C. Mo Incorporation in WO3 Thin Film Photoanodes: Tailoring the Electronic Structure for Photoelectrochemical

Hydrogen Production. *Appl. Phys. Lett.* **2010**, *96* (3), 032107. https://doi.org/10.1063/1.3291689.

(38) Marín, G.; Rincón, C.; Wasim, S. M.; Sánchez Pérez, G.; Molina Molina, I. Temperature Dependence of the Fundamental Absorption Edge in CuGa3Se5. *J. Alloys Compd.* **1999**, *283* (1–2), 1–4. https://doi.org/10.1016/S0925-8388(98)00878-0.

(39) Mezher, M.; Garris, R.; Mansfield, L. M.; Horsley, K.; Weinhardt, L.; Duncan, D. A.; Blum, M.; Rosenberg, S. G.; Bär, M.; Ramanathan, K.; et al. Electronic Structure of the Zn(O,S)/Cu(In,Ga)Se 2 Thin-Film Solar Cell Interface. *Prog. Photovoltaics Res. Appl.* **2016**, *24* (8), 1142–1148. https://doi.org/10.1002/pip.2764.

(40) Hauschild, D.; Meyer, F.; Benkert, A.; Kreikemeyer-Lorenzo, D.; Dalibor, T.; Palm, J.; Blum, M.; Yang, W.; Wilks, R. G.; Bär, M.; et al. Improving Performance by Na Doping of a Buffer Layer-Chemical and Electronic Structure of the In x S Y :Na/CuIn(S,Se) 2 Thin-Film Solar Cell Interface. *Prog. Photovoltaics Res. Appl.* **2018**, *26* (5), 359–366. https://doi.org/10.1002/pip.2993.

(41) Kim, J.; Minegishi, T.; Kobota, J.; Domen, K. Investigation of Cu-Deficient Copper Gallium Selenide Thin Film as a Photocathode for Photoelectrochemical Water Splitting. *Jpn. J. Appl. Phys.* **2012**, *51* (1), 015802. https://doi.org/10.1143/JJAP.51.015802.

(42) Gueymard, C. SMARTS: Simple Model of the Atmospheric Radiative Transfer of Sunshine https://www.nrel.gov/rredc/smarts/ (accessed Nov 3, 2019).

(43) Gueymard, C. *SMARTS2, A Simple Model of the Atmospheric Radiative Transfer of Sunshine: Algorithms and Performance Assessment*; Cocoa, FL, 1995.

(44) Gueymard, C. Parameterized Transmittance Model for Direct Beam and Circumsolar Spectral Irradiance. *Sol. Energy* **2001**, *71*, 325–346.

(45) Hellstern, T. R. *Engineering Catalysts, Interfaces, and Semiconductors for Sustainable Hydrogen Production via Solar Driven Water Splitting*; PhD Thesis, Stanford University, 2017.

(46) Knöppel, J.; Zhang, S.; Speck, F. D.; Mayrhofer, K. J. J.; Scheu, C.; Cherevko, S. Time-Resolved Analysis of Dissolution Phenomena in Photoelectrochemistry – A Case Study of WO3 Photocorrosion. *Electrochem. commun.* **2018**, *96* (September), 53–56. https://doi.org/10.1016/j.elecom.2018.09.008.

(47) Wang, Y.; Schwartz, J.; Gim, J.; Hovden, R.; Mi, Z. Stable Unassisted Solar Water Splitting on Semiconductor Photocathodes Protected by Multifunctional GaN Nanostructures. *ACS Energy Lett.* **2019**, 1541–1548. https://doi.org/10.1021/acsenergylett.9b00549.

(48) Wang, T.; Liu, S.; Li, H.; Li, C.; Luo, Z.; Gong, J. Transparent Ta 2 O 5 Protective Layer for Stable Silicon Photocathode under Full Solar Spectrum. *Ind. Eng. Chem. Res.* **2019**, *58* (14), 5510–5515. https://doi.org/10.1021/acs.iecr.9b00147.

(49) Bae, D.; Pedersen, T.; Seger, B.; Iandolo, B.; Hansen, O.; Vesborg, P. C. K.; Chorkendorff, I. Carrier-Selective p- and n-Contacts for Efficient and Stable Photocatalytic Water Reduction. *Catal. Today* **2017**, *290*, 59–64. https://doi.org/10.1016/j.cattod.2016.11.028.

(50) Tan, C. S.; Kemp, K. W.; Braun, M. R.; Meng, A. C.; Tan, W.; Chidsey, C. E. D.; Ma, W.; Moghadam, F.; McIntyre, P. C. 10% Solar-to-Hydrogen Efficiency Unassisted Water Splitting on ALD-Protected Silicon Heterojunction Solar Cells. *Sustain. Energy Fuels* **2019**. https://doi.org/10.1039/C9SE00110G.

TOC Graphic

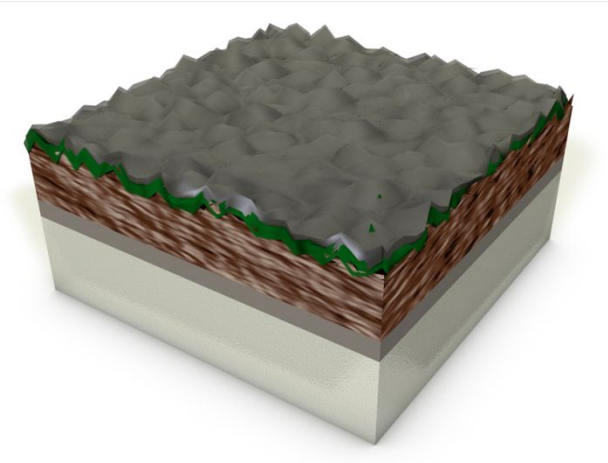

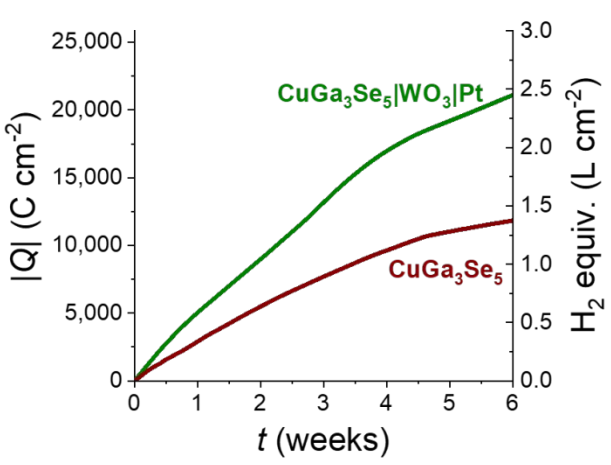
25,000
20,000
15,000
10,000
5,000
0
|Q| (C cm-2)
3.0
2.5
2.0
1.5
1.0
0.5
0.0
H2 equiv. (L cm-2)
0
1
2
3
4
5
6
t (weeks)
CuGa3Se5|WO3|Pt
CuGa3Se5